



Cite this: *RSC Adv.*, 2020, **10**, 13215

## The improved performance and mechanism of solution-processed blue PhOLEDs based on double electron transport layers

Zijian Liu, <sup>ab</sup> WeiYe Zheng, <sup>ab</sup> Peng Wei, <sup>ab</sup> Zheng Xu, <sup>ab</sup> Dandan Song, <sup>ab</sup> Bo Qiao <sup>ab</sup> and Suling Zhao <sup>\*ab</sup>

Performance improved solution-processed blue phosphorescent organic light emitting diodes (PhOLEDs) are demonstrated by adopting a double electron transport layer (ETL) strategy, which consists of TPBi and an additional  $\text{Alq}_3$  ETL. With the help of  $\text{Alq}_3$  ETL, the performance of the optimal device with a double ETL is significantly enhanced. The maximum luminance of OLEDs is improved from  $6787 \text{ cd m}^{-2}$  to  $13\,054 \text{ cd m}^{-2}$ , and the maximum current efficiency is increased from  $3.9 \text{ cd A}^{-1}$  to  $11.4 \text{ cd A}^{-1}$ . Furthermore, the difference of carrier injection in the two types of PhOLEDs is explored by using the transient electroluminescence measurement method. The results imply that double ETL can help to balance electron injection and carrier transport, reduce the interface charge accumulation, leading to a high efficiency. The PL decay of the emission layer with different ETL is detected to analyze the effect of the introduced second ETL layer and the interface on the exciton decay of the emission layer. The results show that the introduced interface in devices with a double ETL has an adverse effect on the exciton emission, which contributes to the serious efficiency roll-off of devices with a double ETL.

Received 18th January 2020

Accepted 14th February 2020

DOI: 10.1039/d0ra00515k

rsc.li/rsc-advances

### 1. Introduction

Organic light-emitting diodes (OLEDs) increasingly attract interest because of their great potential in the field of high-quality flat panel displays and solid-state lightning.<sup>1–4</sup> For these applications, the luminance of OLEDs needs to reach  $1000 \text{ cd m}^{-2}$  (ref. 4–6) and even higher for the solid-state lighting devices.<sup>5,7</sup> At present, the green OLEDs and the red OLEDs have achieved a high efficiency and long lifetime, which are enough for their applications. But how to improve the performance of the blue OLEDs is still a bottleneck, especially for solution-processed blue OLEDs.<sup>8–11</sup>

In blue OLEDs, the electron transport layer (ETL) plays an important role in conducting electrons and blocking holes. Because most blue OLEDs are hole-dominant devices, the selection of appropriate ETL can optimize the electron injection and transportation then balance the carrier and reduce the leakage current to raise the brightness and efficiency of devices.<sup>12</sup> But a poor ETL setting will make electrons difficult to inject, and lead to charge storage in the interface between the emitting layer (EML) and ETL, which may result in the exciton quenching.

Based on this problem, various methods have been investigated. Generally, double ETL has been widely used in various

OLEDs to form a step barrier between the EML and cathode to enhance the electronic injection and improve the device efficiency, which not only avoids the device stability problem caused by mix host doping, but also saves the complex steps of cross-linking materials. In addition, it does not need to develop new host and guest materials, and avoids the defects of mixed evaporation.<sup>13</sup> Yu Bai *et al.* inserted  $\text{Ga}_q$  between  $\text{Alq}_3$  and TBADN to form a double ETL and fabricated blue OLED devices, which resulting in the increase of efficiency.<sup>14</sup> Zhang *et al.* fabricated a blue OLED device using Bpy-OXD/ $\text{Alq}_3$  as a double ETL. The device showed much better chromaticity and less current-induced color shift as compared to the corresponding single ETL ones.<sup>15</sup> Jang *et al.* used an double ETL of Bphen/ $\text{Alq}_3$  to realize a higher current density and luminance.<sup>16</sup> Jia *et al.* demonstrated blue PhOLEDs containing a double ETL with the structure of  $\text{Li}(\text{acac})\text{:PEI/ZnO:PI}$ .<sup>17</sup> This structure markedly improved the electron injection and transport and suppressed the triplet exciton quenching at the EML/ZnO interface, resulting in a lower driving voltage and doubled luminous efficiency compared with those of the control device. However, there is still a lack of an double ETL suitable for solution-processed 3,3'-bis(*N*-carbazolyl)biphenyl (mcp) system blue OLEDs.

In this paper, the double ETL structure of 1,3,5-tris(1-phenyl-1*H*-benzimidazol-2-yl)benzene (TPBi)/tris-(8-hydroxyquinoline) aluminum ( $\text{Alq}_3$ ) was introduced into the solution-processed blue PhOLEDs based on 3,3'-bis(*N*-carbazolyl)biphenyl:bis[(4,6-difluorophenyl)-pyridine-to-N,C<sub>2</sub>](picolinate) iridium(III)

<sup>a</sup>Key Laboratory of Luminescence and Optical Information, Beijing Jiaotong University, Ministry of Education, Beijing 100044, China

<sup>b</sup>Institute of Optoelectronics Technology, Beijing Jiaotong University, Beijing 100044, China



(mcp:Firpic) emitting layer (EML) in order to optimize the electron injection and expand the recombination region of excitons. Therefore, both the triplet-triplet annihilation (TTA) and triplet polaron quenching (TPQ) are expected to be restrained, which will improve the performance of the solution-processed blue PhOLED device.<sup>18-22</sup> Therefore, to select two ETL materials for matching the energy barrier is a key issue to improve the electron injection and transport. The energy barrier between TPBi and cathode is 1.1 eV before introducing Alq<sub>3</sub>, and the electron injection barrier is reduced to 0.8 eV after the addition of Alq<sub>3</sub>,<sup>16,23-25</sup> which can promote electron injection and balance charge carriers. The max luminance ( $L_{\max}$ ) of 13 054 cd m<sup>-2</sup> and the max current efficiency (CE<sub>max</sub>) of 11.4 cd A<sup>-1</sup> are achieved in the optimal double ETL device, and at the luminance of 1000 cd m<sup>-2</sup>, the efficiency still maintain at 10.8 cd A<sup>-1</sup>. Compared with the single ETL device ( $L_{\max}$  is 6787 cd m<sup>-2</sup>, CE<sub>max</sub> is 3.9 cd A<sup>-1</sup>), the double ETL system has done well in improving the performance of solution-processed blue

OLED. Then the transient electroluminescence measurement was used to detect the carrier injection, capture and accumulation in the devices.

## 2. Experimental details

## Materials

The hole-injection material of poly(3,4-ethylenedioxythiophene):poly (styrene sulfonate) (PEDOT:PSS), the host material of mcp, the electron-transporting material of TPBi and Alq<sub>3</sub>, and the phosphorescent dopant of Firpic are all purchased from Xi'an p-oled Optoelectronics Technology Co. Ltd. The molecular structures of mcp, Firpic and Alq<sub>3</sub> are shown in Fig. 1.

## Device fabrication

The energy level structure of the double ETL solution-processed blue OLED is shown in Fig. 2a and b. The glass substrates with patterned ITO were cleaned by ultrasonic bath with detergent.

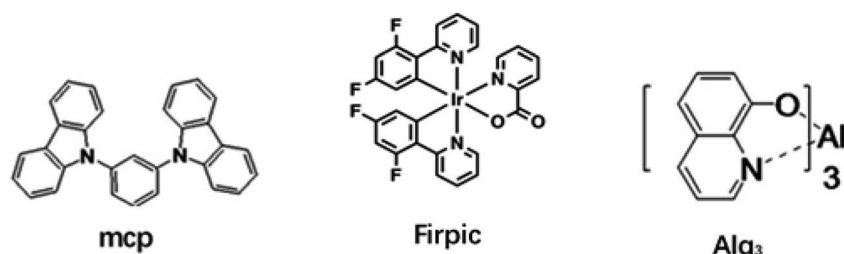


Fig. 1 Molecular structures of mcp, Firpic and Alaq<sub>3</sub>

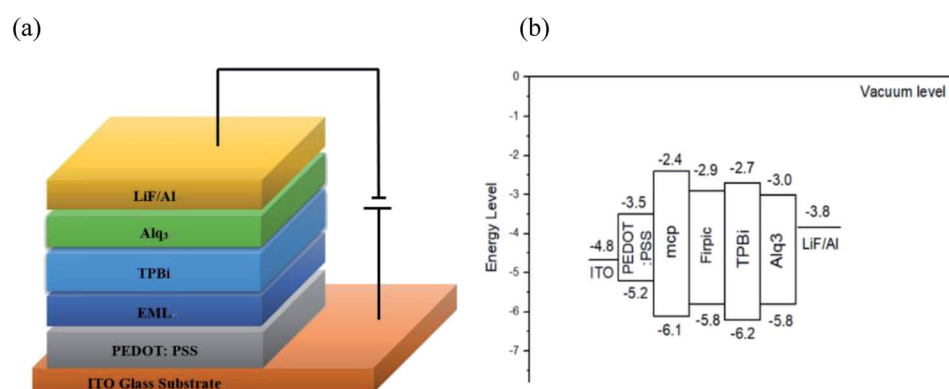


Fig. 2 (a) Device structure of the OLEDs and (b) energy level diagram of the OLEDs

**Table 1** The device performances of OLEDs based on single ETL TPBi with different thicknesses

Devices	Thickness of TPBi (nm)	Turn-on (V)	$L_{\max}$ (cd m $^{-2}$ )	$CE_{\max}$ (cd A $^{-1}$ )	$EQE_{\max}$ (%)	Color coordinates <sup>a</sup>	Peak wavelength <sup>b</sup> (nm)
1	20	3.6	3158	2.1	1.0	(0.15, 0.36)	471
2	25	3.6	4043	3.6	1.7	(0.15, 0.36)	472
3	30	3.6	4857	4.9	2.3	(0.15, 0.36)	471
4	35	3.6	5185	7.4	3.3	(0.16, 0.37)	472

<sup>a</sup> The color coordinates at 1000 cd m<sup>-2</sup>. <sup>b</sup> The peak wavelength at 1000 cd m<sup>-2</sup>.

deionized water, and alcohol successively for 20 minutes each. Then they were dried with nitrogen flow and treated in plasma treatment for 90 s. The hole injection layer (HIL) of PEDOT:PSS was spin-coated on the ITO glass substrate at 4000 rpm and then baked at 150 °C for 15 min to remove residual moisture. Afterwards, all samples were moved into the glovebox. The EML materials of mcp and Firpic were separately dissolved in the solvent of chlorobenzene and then mixed in a specific ratio. In the glovebox, the mixed solution of mcp and Firpic was spin-coated at 3000 rpm on the HIL as an emitting layer and then baked at 60 °C for 25 min to remove residual solvent. Then the electron transport layer (ETL) of TPBi/Alq<sub>3</sub> and the cathode of LiF/Al were thermally evaporated under a pressure of below 1 × 10<sup>-4</sup> Pa.

### Characterization

The current–voltage–luminance (*J*–*V*–*L*) characteristics and electroluminescence (EL) spectrum of these devices were measured by a test system which consist of computer, Keithley 2410 and SRC-600 spectral radiance colorimeter; transient electroluminescence (TREL) was measured by a transient illuminating test system which consist of a signal generator, a timing controller, a photomultiplier tube and an oscilloscope. The transient photoluminescence (TRPL) was tested using the Horiba Instrument FluoroCube01-N1. All measurements were made under air conditions.

## 3. Results and discussions

Due to the property of high triplet energy level (3.02 eV) and good solubility, mcp is appropriate to be used as the host material for solution-processed blue PhOLED. So firstly in this paper, we chose mcp as the host and Firpic as the dopant to prepare a set of devices with the structure of ITO/PEDOT:PSS/mcp:16 wt% Firpic/TPBi (*X* nm)/LiF (0.7 nm)/Al (100 nm) by changing the thickness of only one ETL for optimize the electron injection. *X* is equal to 20 nm, 25 nm, 30 nm, and 35 nm, respectively. The results shows that the luminance and current efficiency of devices increases with the increasing thickness of the ETL, and the turn-on voltage also increases slightly, but the current density of the device decreases as the thickness increases. As shown in Table 1, the *L*<sub>max</sub> of the device with 35 nm ETL achieves to 5185 cd m<sup>-2</sup>, while the CE<sub>max</sub> achieves to 7.4 cd A<sup>-1</sup> and the turn-on voltage is kept at a relatively low level of 3.6 V, which slightly exceeds the best performance of similar devices in ref. 26. As shown in Fig. 1b, the electron injection barrier between TPBi and Al cathode is 1.1 eV, which is too large to inject electron easily and results in electrons accumulation at the TPBi/Al interface. In addition, because the hole mobility ( $\mu_h \approx 1.2 \times 10^{-4} \text{ cm}^2 \text{ V}^{-1} \text{ s}^{-1}$ ) of mcp is much larger than the electron mobility ( $\mu_e \approx 5.1 \times 10^{-6} \text{ cm}^2 \text{ V}^{-1} \text{ s}^{-1}$ ), the majority carrier in the device is hole. Therefore, the device performance depends greatly on the electrons injected to the emission layer. Since the lowest unoccupied molecular orbital (LUMO) of Alq<sub>3</sub> is deeper than TPBi, if Alq<sub>3</sub> is used as the second electron transport layer, the electron injection barrier can be effectively

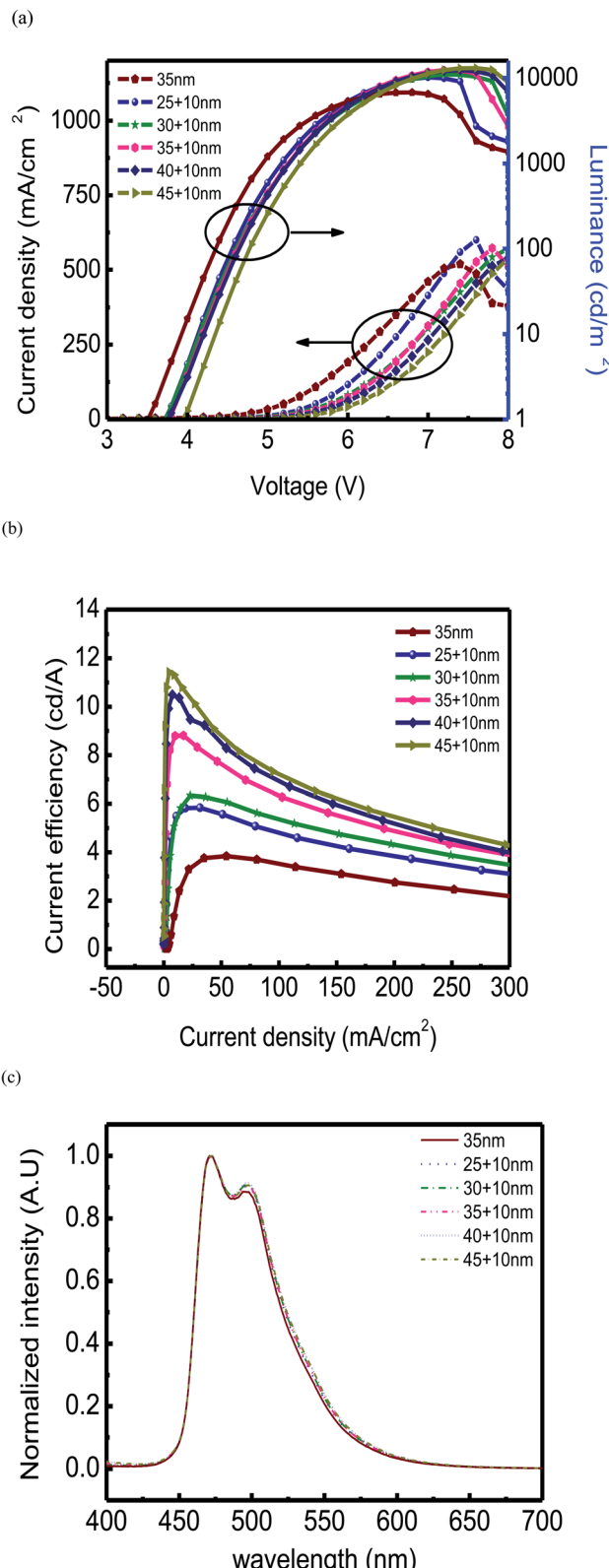


Fig. 3 (a) Current–voltage–luminance (*J*–*V*–*L*) of OLEDs based on different thickness of single and double ETL. (b) Current efficiency of OLEDs based on single and double ETL. (c) Electroluminescence spectra of the blue PhOLEDs.



Table 2 The device performances of OLEDs based on single ETL TPBi and double ETL TPBi/Alq<sub>3</sub> with different thickness

Devices	Thickness of TPBi (nm)	Thickness of Alq <sub>3</sub> (nm)	Turn-on (V)	L <sub>max</sub> (cd m <sup>-2</sup> )	CE <sub>max</sub> (cd A <sup>-1</sup> )	EQE <sub>max</sub> (%)	Color coordinates <sup>a</sup>	Peak wavelength <sup>b</sup> (nm)
1	35	0	3.6	6787	3.9	1.9	(0.15, 0.35)	472
2	25	10	3.7	10 187	5.9	2.8	(0.15, 0.35)	471
3	30	10	3.7	10 986	6.4	3.0	(0.15, 0.35)	471
4	35	10	3.8	12 424	8.7	4.2	(0.15, 0.35)	472
5	40	10	3.8	12 346	10.6	5.0	(0.15, 0.35)	473
6	45	10	4.1	13 054	11.4	5.5	(0.15, 0.35)	473

<sup>a</sup> The color coordinates at 1000 cd m<sup>-2</sup>. <sup>b</sup> The peak wavelength at 1000 cd m<sup>-2</sup>.

reduced from 1.1 eV to 0.8 eV.<sup>16,27</sup> Therefore, we prepared OLEDs with a additional 10 nm ETL of Alq<sub>3</sub>, to reduce the electron injection barrier and explore the effect of thickness of TPBi on the device performance.

A series of devices with ITO/PEDOT:PSS/mcp:16 wt% Firpic/TPBi (X nm)/Alq<sub>3</sub> (0 or 10 nm)/LiF (0.7 nm)/Al (100 nm) structures were fabricated, the thickness X of TPBi is 25 nm, 30 nm, 35 nm, 40 nm and 45 nm, respectively. The turn-on voltage of the double ETL system device is slightly higher as expected, and the brightness and efficiency are improved greatly. It is because that the introduction of Alq<sub>3</sub> with a LUMO of 3.0 eV reduces the electron injection barrier and makes it easier for electrons inject into the EML, which helps to balance carriers. And the slightly increasing of turn-on voltage of the device may be due to the interface effect or the increasing thickness of whole EML as shown in Fig. 3a and b. Fig. 3c shows the EL spectrum of different blue OLEDs. All devices exhibit only Firpic emissions centered at 472 nm. As shown in Table 2, the TPBi/Alq<sub>3</sub> device achieves a L<sub>max</sub> of 13 054 cd m<sup>-2</sup> and a CE<sub>max</sub> of 11.4 cd A<sup>-1</sup>, and at the luminance of 1000 cd m<sup>-2</sup>, the efficiency still maintain at 10.8 cd A<sup>-1</sup>, which is significantly higher than that of the device with a single ETL of TPBi whose L<sub>max</sub> is 6787 cd m<sup>-2</sup> and CE<sub>max</sub> is 3.9 cd A<sup>-1</sup>.

In order to study the effect of double ETL devices on the electron injection, a group of devices based on holes and electrons were fabricated to analyse the transfer mechanism of carriers.<sup>28–30</sup> The devices structure is shown in Table 3. It can be seen from Fig. 4 that the hole current of device 1 is much larger than the electron current of device 2. It means that the electrons and holes inside the EML of the PhOLEDs only with TPBi as the ETL do not match. After introduced Alq<sub>3</sub> as the second ETL, the electron current has been much improved greatly in device 3 compared with device 2, which indicates that the introduction of the second electron transport layer Alq<sub>3</sub> helps to reduce the electron injection barrier and optimize the carrier balance.

Through transient electroluminescence measurements, the mechanism of carrier transport, accumulation, capture and even mobility in organic light-emitting devices (OLEDs)<sup>31–33</sup> could be analyzed. So we introduced the transient electroluminescence measurement to observe the internal carrier movement of the device and analyze the effect of double ETL. The experimental device of transient electroluminescence measurement and the timing setting of the driving voltage are

shown in Fig. 5a. The single ETL device and the double ETL device with the thickness of 35 nm were detected for their transient electroluminescence characteristic curve by applying a voltage pulse with a pulse width of 0.5 ms. The pulse width is sufficient to achieve their steady-state driving. The transient electroluminescence characteristic curve can be seen from Fig. 5b. When a pulse is applied, the double ETL device first reaches its steady-state light emission under the same driven pulse as shown in Fig. 5c, which indicates that the electron injection and transport is improved after the introduction of the second ETL Alq<sub>3</sub>.

When the bias is turned off, as shown in Fig. 5d, the device is still luminous and exhibits an instantaneous overshoot peak that is stronger than the steady state. The transient overshoot refers to the phenomenon that the luminous intensity suddenly

Table 3 Structure of single carrier devices

Devices	Device type	Device structure
1	Hole-only	ITO/PEDOT/mcp:Firpic (16 wt%)/MoO <sub>3</sub> /LiF/Al
2	Electron-only	ITO/ZnO/mcp:Firpic (16 wt%)/TPBi/LiF/Al
3	Electron-only	ITO/ZnO/mcp:Firpic (16 wt%)/TPBi/Alq <sub>3</sub> /LiF/Al

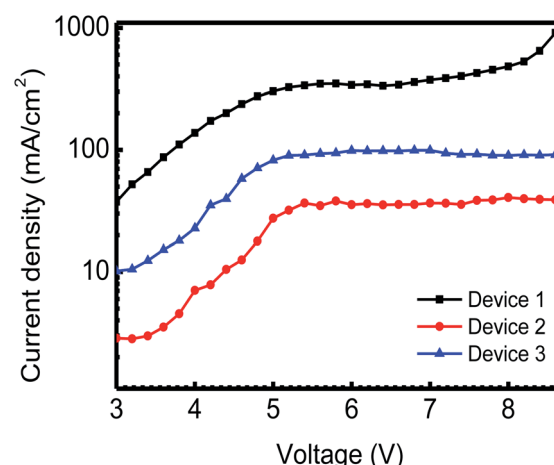


Fig. 4 Current density–voltage characteristics in the hole-dominated devices ITO/PEDOT/mcp:Firpic (16 wt%)/MoO<sub>3</sub>/LiF/Al and the electron-dominated devices ITO/ZnO/mcp:Firpic (16 wt%)/TPBi/LiF/Al and ITO/ZnO/mcp:Firpic (16 wt%)/TPBi/Alq<sub>3</sub>/LiF/Al.



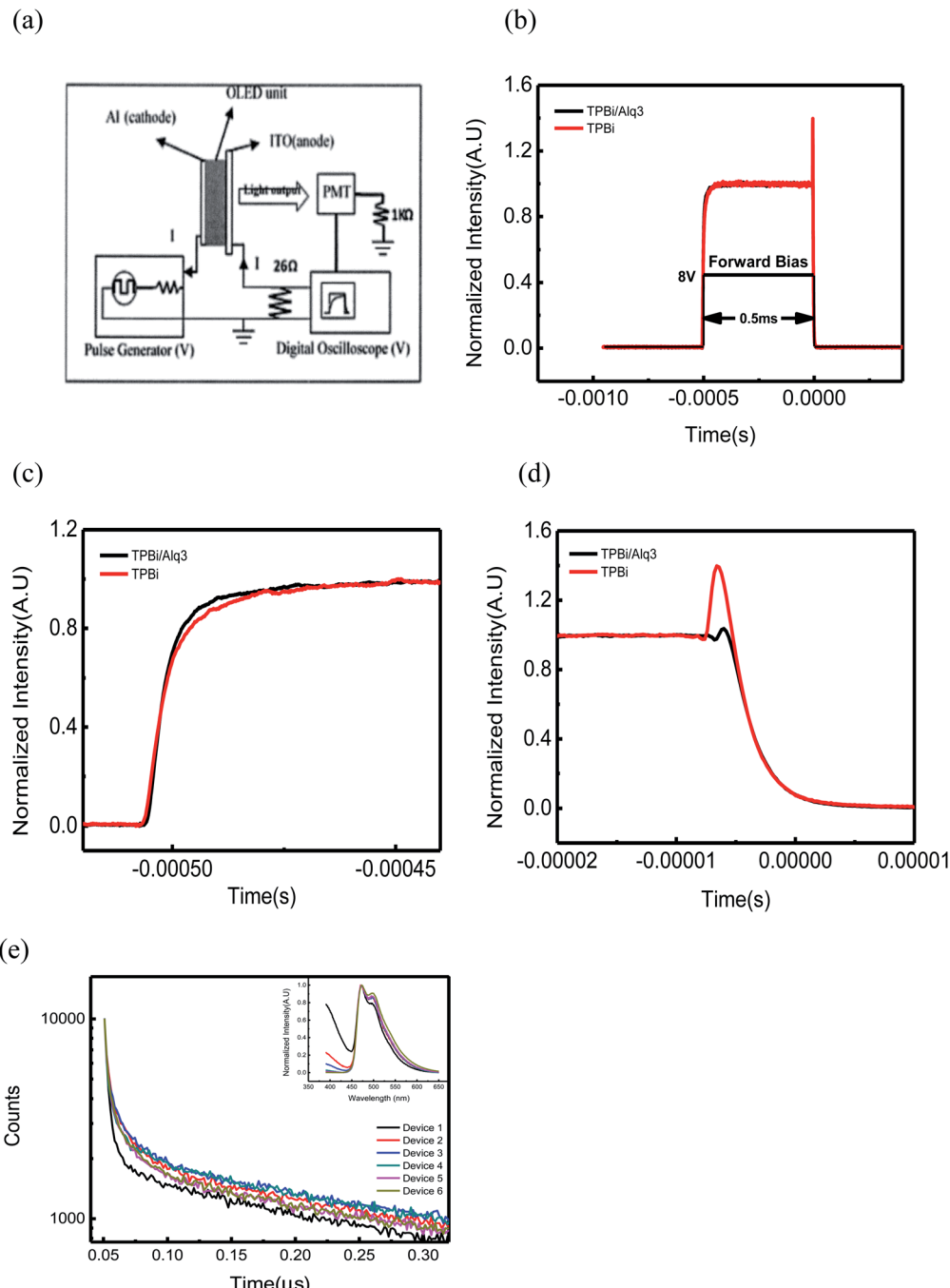


Fig. 5 (a) The experimental device of transient electroluminescence measurement, (b) the transient electroluminescence characteristics and the timing setting of the driving voltage, (c) the transient electroluminescence rising edge characteristic curve, (d) the transient electroluminescence overshoot characteristic curve of the devices based on single and double ETL structure under a periodic electrical pulse of 8 V, 0.5 ms, (e) the PL decay detected in the side of ETL under the excitation of 340 nm of the devices based on single and double ETL structure.

exceeds the steady state a few microsecond after turn off the driving bias, which could be resulted from the recombination of carriers stored in traps or near the interface which accumulated under application of positive bias.<sup>32-34</sup> The transient overshoot is strongly dependent, among other parameters, on device materials and structure. Rui Liu *et al.* reported that the spikes are significantly weaker in devices where a Bphen ETL-HBL layer is added, likely due to enhanced electron transport, and

absent in devices where MoO<sub>3</sub> replaces CuPc.<sup>32</sup> As shown in Fig. 5d, the transient overshoot peak decreases significantly with the addition of the second ETL. From the energy level structure in Fig. 1, the energy barrier between TPBi and the cathode Al reaches 1.1 eV, it is difficult for electrons to jump from the cathode to TPBi and causes a large number of electrons accumulated at the interface. When Alq<sub>3</sub> is added, the energy barrier is reduced to 0.8 eV, and the instantaneous



Table 4 Structure of PL decay devices

EML Structure	
1	Quartz substrate/mcp:Firpic (16 wt%)/TPBi (35 nm)
2	Quartz substrate/mcp:Firpic (16 wt%)/TPBi (25 nm)/Alq <sub>3</sub> (10 nm)
3	Quartz substrate/mcp:Firpic (16 wt%)/TPBi (20 nm)/Alq <sub>3</sub> (15 nm)
4	Quartz substrate/mcp:Firpic (16 wt%)/TPBi (15 nm)/Alq <sub>3</sub> (20 nm)
5	Quartz substrate/mcp:Firpic (16 wt%)/TPBi (10 nm)/Alq <sub>3</sub> (25 nm)
6	Quartz substrate/mcp:Firpic (16 wt%)/TPBi (5 nm)/Alq <sub>3</sub> (30 nm)

overshoot peak is greatly reduced. Therefore, it is concluded that the intensity of the overshoot peak is mainly affected by the electrons stored at the interface. In a single ETL device, when the bias is turned off, the electrons accumulated at the TPBi/cathode interface are released to form excitons with the holes inside the emission layer. These excitons give the overshoot emission and delayed emissions. The addition of the second layer of ETL provides an energy level gradient, which reduces the electron injection barrier and the amount of charge stored at the interface. So the transient overshoot is reduced. The stored charges act as polarons and interact with excitons. The energy could transfer from the triplet exciton to the polaron results in nonradiative recombination. The more charges store in devices, the stronger the interaction between excitons and polarons is. The stronger interaction of exciton–polarons will fast the decay of excitons and reduces the electroluminescence efficiency. Especially under the high current, the stored charges increase greatly, and the efficiency decrease greatly. However, another introduced interface inside the double ETL will results in more defects inside ETL, which attributes more seriously efficiency roll-off in devices. The PL decay of the emission layer with different ETL prove it further.

The emission layer (EML) were fabricated on quartz substrates with the structure of quartz substrate/mcp:Firpic (16 wt%)/ETL (35 nm) were prepared and the PL decay was detected in the side of ETL under the excitation of 340 nm to analyze the effect of an introduced the second ETL layer and the interface on the exciton decay of the emission layer. As shown in Table 4, the distance of the interface between TPBi and Alq<sub>3</sub> is different by changing the thickness of TPBi and Alq<sub>3</sub>. The PL spectra of all films come from the emission of Firpic mainly, as shown as the inset in Fig. 5e. The main PL peak locates at 472 nm corresponding to the exciton recombination of Firpic, and the emission of TPBi was also detected as a tail in the short wavelength. Then the PL decay monitored at 472 nm was detected as shown in Fig. 5e. The PL of Firpic with a single ETL decays faster than that of Firpic with a double ETL. It means that the double ETL is favour to the exciton formation and emit if the exciton zone in the emission layer was considered to be same for different structures. The thicker TPBi is, the more excitation light will be absorbed by TPBi, and the absorption of mcp will decrease, which can be proved by the different PL intensity of TPBi. The results is that the energy transfer from thicker TPBi to Firpic will be weaker because of the long distance from TPBi molecular around its surface to Firpic. The energy transfer probability from the host to Firpic is

considered to be same. Therefore, the slower decay of PL with a double ETL will be attributed to the thinner of TPBi which increases the host absorption and the energy transfer probability from TPBi to Firpic. In such case, the number of excitons formed in the emission layer under 340 nm excitation increases along with the thinner of TPBi and reaches the maximum when TPBi is 20 nm. Although the thinner TPBi helps to transfer energy from TPBi to Firpic and increases the number of Firpic excitons, the interface in where there are more defects closes to the emission layer. The interaction between excitons of Firpic and these defects will de-excite nonradiatively the excitons of Firpic. When the thickness of TPBi decreases, the quenching caused by the interface defects is enhanced,<sup>35–37</sup> and the PL decay becomes faster again. So it is concluded that the interface is adverse to the exciton emission. Therefore, as shown in Fig. 3b, the efficiency roll-off of devices with a double ETL is more serious than with a single ETL, even the electron injection is improved in devices with double ETL.

## 4. Conclusions

In summary, compared with the single ETL device, the current efficiency and luminance of the blue phosphorescent device prepared by the solution method of TPBi and Alq<sub>3</sub> as a double ETL have been improved. By studying hole-only and electron-only devices, it is found that the addition of Alq<sub>3</sub> optimizes the carrier balance. Transient electroluminescence measurement shows that the addition of Alq<sub>3</sub> reduces transient overshoot. The results shows that the small spikes of transient overshoot mainly come from the electrons accumulated in the interface between the TPBi and cathode. Therefore, the addition of Alq<sub>3</sub> reduces the electron injection barrier and optimizes the device performance to achieve an optimized  $CE_{max}$  to 11.4 cd A<sup>-1</sup>,  $L_{max}$  of 13 054 cd m<sup>-2</sup>. At the luminance of 1000 cd m<sup>-2</sup>, the efficiency still maintain at 10.8 cd A<sup>-1</sup>, which is significantly higher than that of a single ETL device. The introduced interface in devices with a double ETL has an adverse effect on the exciton emission according to the results of PL decay measurements, which attributes to the serious efficiency roll-off of devices with a double ETL. Hence, it is necessary to optimize the interface effect further in solution-processed PhOLEDs.

## Conflicts of interest

There are no conflicts to declare.

## Acknowledgements

The authors express the thanks to the National Key Research and Development Program of China under Grant No. 2016YFB0401302 and the National Natural Science Foundation of China under Grant No. 61704007 and No. 61775013.

## References

- 1 C. W. Tang and S. A. VanSlyke, Organic electroluminescent diodes, *Appl. Phys. Lett.*, 1987, **51**, 913–915.



2 C. W. Tang, S. A. VanSlyke and C. H. Chen, Electroluminescence of doped organic thin films, *J. Appl. Phys.*, 1989, **65**, 3610–3616.

3 S. Ameen, J. Lee, H. Han, M. Suh and C. Lee, Curing temperature reduction and performance improvement of solution-processable hole-transporting materials for phosphorescent OLEDs by manipulation of cross-linking functionalities and core structures, *RSC Adv.*, 2016, **6**, 33212–33220.

4 M. McCarthy, B. Liu, E. Donoghue, I. Kravchenko, D. Kim, F. So and A. Rinzler, Low-Voltage, LowPower, Organic Light-Emitting Transistors for Active Matrix Displays, *Science*, 2011, **332**, 570–573.

5 H. Wu, G. Zhou, J. Zou, C. Ho, W. Wong, W. Yang, J. Peng and Y. Cao, Efficient Polymer White-Light Emitting Devices for Solid-State Lighting, *Adv. Mater.*, 2009, **21**, 4181–4184.

6 J. Jou, K. Chou, F. Yang, C. Hsieh, S. Kumar, A. Agrawal, S. Chen, T. Li and H. Yu, Pseudo-Natural Light for Displays and Lighting, *Adv. Opt. Mater.*, 2015, **3**, 95–102.

7 J. Kim, C. Joo, J. Lee, J. Woo, J. Oh, N. Baek, H. Chud and J. Lee, Save energy on OLED lighting by a simple yet powerful technique, *RSC Adv.*, 2015, **5**, 8415–8421.

8 E. Kozma, W. Mróz, F. Villafiorita-Monteleone, F. Galeotti, A. Andicsová-Eckstein, M. Catellania and C. Botta, Perylene diimide derivatives as red and deep red-emitters for fully solution processable OLEDs, *RSC Adv.*, 2016, **6**, 61175–61179.

9 C. Adachi, M. Baldo and S. R. Forrest, High-efficiency red electrophosphorescence devices, *Appl. Phys. Lett.*, 2001, **78**, 1622–1624.

10 X. Liu, S. Wang, B. Yao, B. Zhang, C. Ho, W. Wong, Y. Cheng and Z. Xie, New deep-red heteroleptic iridium complex with 3-hexylthiophene for solution-processed organic light-emitting diodes emitting saturated red and high CRI white colors, *Org. Electron.*, 2015, **21**, 1–8.

11 S. Ye, T. Hu, Z. Zhou, M. Yang, M. Quan, Q. Mei, B. Zhai, Z. Jia, W. Lai and W. Huang, Solution processed single-emission layer white polymer light-emitting diodes with high color quality and high performance from a poly(N-vinyl)carbazole host, *Phys. Chem. Chem. Phys.*, 2015, **17**, 8860–8869.

12 N. Chopra, J. Lee, Y. Zheng, S. Eom, J. Xue and F. So, Effect of the charge balance on high-efficiency blue-phosphorescent organic light-emitting diodes, *ACS Appl. Mater. Interfaces*, 2009, **1**, 1169–1172.

13 B. Sim, C. Moon, K. Kim and J. Kim, Quantitative Analysis of the Efficiency of OLEDs, *ACS Appl. Mater. Interfaces*, 2016, **8**, 33010–33018.

14 Y. Bai, M. Khan, W. Zhu, X. Jiang and Z. Zhang, A blue organic light emitting diodes with graded junction, *Displays*, 2008, **29**, 365–368.

15 X. Zhang, J. Li, M. Khan, L. Zhang, X. Jiang, K. Haq, W. Zhu and Z. Zhang, Improved chromaticity and electron injection in a blue organic light-emitting device by using a dual electron-transport layer with hole-blocking function, *Semicond. Sci. Technol.*, 2009, **24**, 075021.

16 J. Jang, H. Ji, H. Kim and J. Jeong, TPBI:FIrpic organic light emitting devices with the electron transport layer of Bphen/Alq<sub>3</sub>, *Curr. Appl. Phys.*, 2011, **11**, S251–S254.

17 M. Jia, X. Xu, J. Peng, J. Zhang, C. Yao and L. Li, Solution-Processed Double-Layer Electron-Transport Layer for Conventional Blue Phosphorescent Organic Light-Emitting Diodes, *Adv. Opt. Mater.*, 2016, **4**, 1635–1641.

18 W. Staroske, M. Pfeiffer, K. Leo and M. Hoffmann, Single-Step Triplet-Triplet Annihilation: an Intrinsic Limit for the High Brightness Efficiency of Phosphorescent Organic Light Emitting Diodes, *Phys. Rev. Lett.*, 2007, **98**, 197402–197406.

19 D. Song, S. Zhao, Y. Luo and H. Aziz, Causes of Efficiency Roll-Off in Phosphorescent Organic Light Emitting Devices: Triplet-triplet Annihilation versus Triplet-Polaron Quenching, *Appl. Phys. Lett.*, 2010, **97**, 243304–243307.

20 B. Minaev, V. Minaeva and H. Ågren, Theoretical Study of the Cyclometalated Iridium(III) Complexes Used as Chromophores for Organic Light-Emitting Diodes, *J. Phys. Chem. A*, 2009, **113**, 726–735.

21 B. Minaev, G. Baryshnikov and H. Agren, Principles of phosphorescent organic light emitting devices, *Phys. Chem. Chem. Phys.*, 2014, **16**, 1719–1758.

22 G. Baryshnikov, B. Minaev and H. Ågren, Theory and Calculation of the Phosphorescence Phenomenon, *Chem. Rev.*, 2017, **117**, 6500–6537.

23 S. Perumal, B. Minaev and H. Ågren, Triplet State Phosphorescence in Tris(8-hydroxyquinoline) Aluminum Light Emitting Diode Materials, *J. Phys. Chem. C*, 2013, **117**, 3446–3455.

24 M. Halls and H. Schlegel, Molecular Orbital Study of the First Excited State of the OLED Material Tris(8-hydroxyquinoline) aluminum(III), *Chem. Mater.*, 2001, **13**, 2632–2640.

25 H. Nakanotani, T. Higuchi, T. Furukawa, K. Masui, K. Morimoto, M. Numata, H. Tanaka, Y. Sagara, T. Yasuda and C. Adachi, High-efficiency organic light-emitting diodes with fluorescent emitters, *Nat. Commun.*, 2014, **5**, 4016.

26 J. Jou, W. Wang, S. Chen, J. Shyue, M. Hsu, C. Lin, S. Shen, C. Wang, C. Liu, C. Chen, M. Wud and S. Liu, High-efficiency blue organic light-emitting diodes using a 3,5-di(9H-carbazol-9-yl)tetraphenylsilane host via a solution-process, *J. Mater. Chem.*, 2010, **20**, 8411–8416.

27 P. Wei, S. Zhao, Z. Xu, D. Song, B. Qiao, P. Wang and J. Yang, Improved carrier injection and balance in solution-processed blue phosphorescent organic light emitting diodes based on mixed host system and their transient electroluminescence, *Synth. Met.*, 2019, **252**, 15–20.

28 Y. Zhao, R. Chen, Y. Gao, K. Leck, X. Yang, S. Liu, A. Abiyasa, Y. Divayana, E. Mutlugun, S. Tan, H. Sun, H. Demir and X. Sun, AC-driven, color- and brightness-tunable organic light-emitting diodes constructed from an electron only device, *Org. Electron.*, 2013, **14**, 3195–3200.

29 A. Kyaw, X. Sun, C. Jiang, G. Lo, D. Zhao and D. Kwong, An inverted organic solar cell employing a sol-gel derived ZnO electron selective layer and thermal evaporated MoO<sub>3</sub> hole selective layer, *Appl. Phys. Lett.*, 2008, **93**, 221107.



30 D. Zhao, X. Sun, C. Jiang, A. Kyaw, G. Lo and D. Kwong, Efficient tandem organic solar cells with an Al/MoO<sub>3</sub> intermediate layer, *Appl. Phys. Lett.*, 2008, **93**, 083305.

31 Y. Luo and H. Aziz, Correlation between triplet triplet annihilation and electroluminescence efficiency in doped fluorescent organic light-emitting devices, *Adv. Funct. Mater.*, 2010, **20**, 1285–1293.

32 R. Liu, Z. Gan, R. Shinar and J. Shinar, Transient electroluminescence spikes in small molecular organic light-emitting diodes, *Phys. Rev. B: Condens. Matter Mater. Phys.*, 2011, **83**, 245302.

33 C. Zhang, B. Qiao, S. Zhao, Z. Xu, P. Wang, Y. Chen, F. Yin, G. Teyssedre, C. Laurent and X. Xu, Transient analysis on stored charges in organic light-emitting diodes and their application in alternating current driven electroluminescence, *Org. Electron.*, 2016, **39**, 348–353.

34 J. Pommerehne, D. Nikolaenkov, V. Nikitenko and H. Bässler, Overshoot effect in transient electroluminescence from single layer organic light-emitting diodes, *J. Appl. Phys.*, 2001, **90**, 5554–5560.

35 J. Lupton, V. Nikitenko and I. Samuel, Time delayed electroluminescence overshoot in single layer polymer light-emitting diodes due to electrode luminescence quenching, *J. Appl. Phys.*, 2001, **89**, 311–317.

36 J. Kalinowski, W. Stampor, J. Męzyk, M. Cocchi, D. Virgili, V. Fattori and P. Marco, Quenching effects in organic electrophosphorescence, *Phys. Rev. B: Condens. Matter Mater. Phys.*, 2002, **66**, 235321.

37 D. Kondakov, J. Sandifer and C. W. Tang, Nonradiative recombination centers and electrical aging of organic light-emitting diodes: direct connection between accumulation of trapped charge and luminance loss, *J. Appl. Phys.*, 2003, **93**, 1108–1119.

